

WEAK FERROMAGNETISM IN AN ANTIFERROMAGNETIC  $\text{CoCO}_3$  SINGLE CRYSTAL

A. S. BOROVIK-ROMANOV and V. I. OZHOGIN

Institute for Physical Problems, Academy of Sciences, U.S.S.R.

Submitted to JETP editor February 13, 1960

J. Exptl. Theoret. Phys. (U.S.S.R.) 39, 27-36 (July, 1960)

The magnetic properties of a  $\text{CoCO}_3$  single crystal were studied at temperatures from 1.3 to 300°K by means of a magnetic balance. In agreement with earlier results,<sup>1</sup> antiferromagnetic ordering with weak ferromagnetism is established in  $\text{CoCO}_3$  below  $T_N = 18.1^\circ\text{K}$ . Some properties differing from the data for  $\text{MnCO}_3$ <sup>4</sup> are the very large anisotropy of the paramagnetic susceptibility, the large spontaneous ferromagnetic moment ( $\sigma_0 = 1440$  cgs emu/mole) and the sharp peak of  $\chi_\perp$  near  $T_N$ . It is shown that the latter feature, can be explained within the thermodynamic theory of weak ferromagnetism,<sup>3</sup> and is associated with the fact that a magnetic field imposed on a disordered substance induces antiferromagnetic ordering.

The anomaly observed in the temperature dependence of the spontaneous moment at low temperatures can be explained within the framework of the spin-wave theory as a transition from the excitation of a single branch to the excitation of both branches of the spin-wave spectrum. As in the case of  $\text{MnCO}_3$ ,<sup>4</sup> no quantitative agreement with the spin-wave theory is observed.

## 1. INTRODUCTION

WEAK ferromagnetism has been observed in polycrystalline samples of manganese and cobalt carbonates.<sup>1</sup> The antiferromagnetism of  $\text{MnCO}_3$  has been confirmed directly by means of neutron diffraction.<sup>2</sup> A detailed theoretical investigation by Dzyaloshinskii<sup>3</sup> and the study of the magnetic properties of  $\text{MnCO}_3$  single crystals<sup>4</sup> have revealed several interesting properties of antiferromagnets possessing weak ferromagnetism.

The character of the orbital level splitting of the cobalt ion in the crystalline field results in a large value for the anisotropy energy that is due to spin-orbit interaction. A detailed investigation of weak ferromagnetism in a  $\text{CoCO}_3$  single crystal was therefore of interest, since the spin-orbit interaction is responsible for this weak ferromagnetism<sup>5,6</sup> and larger effects could be expected together with the appearance of finer details. It was also important to verify an earlier conclusion<sup>4</sup> that the existing theory of spin waves requires correction.

## 2. APPARATUS AND SAMPLES

The magnetic moments of the samples were measured by the Faraday technique using the magnetic balance that is described in reference

7. The apparatus was improved in two ways.\* Oil damping of the balance was replaced by an electronic technique. In order to correct for the torsion of the sample, which was attached to the balance arm by means of a quartz fiber, a device for measuring the angle of rotation was positioned around the vertical axis. This is very important for corrections in measuring the magnetic susceptibility of  $\text{CoCO}_3$  along the trigonal axis, since the very large anisotropy of magnetic properties in this case results in rotations up to  $3^\circ$ .

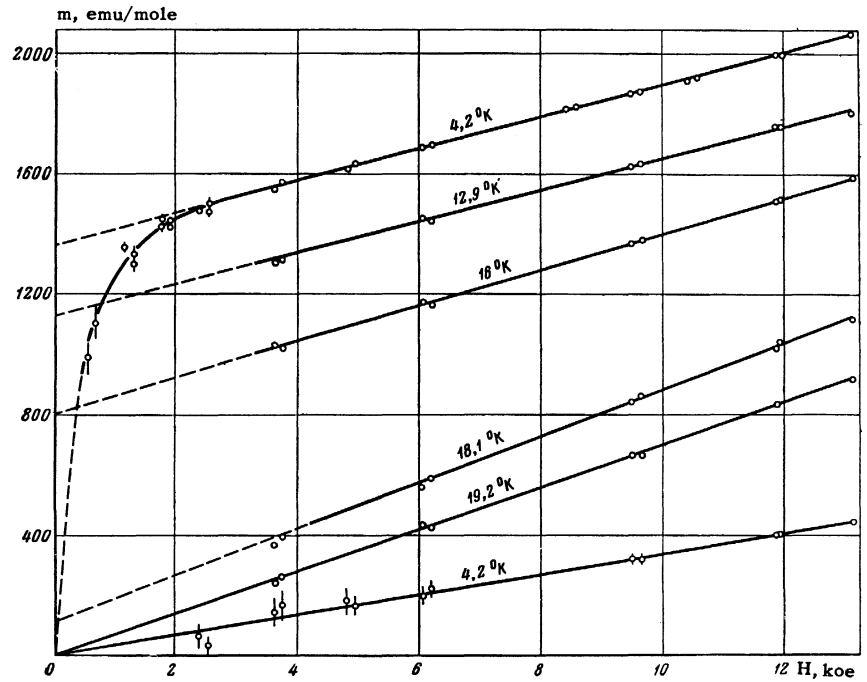
Measurements were performed on single crystals grown hydrothermally by N. Yu. Ikornikova of the Institute of Crystallography, Academy of Sciences U.S.S.R. Cobalt carbonate is isomorphic with  $\text{MnCO}_3$  and possesses a rhombohedral structure with two ions in its unit cell. Each crystal was a smooth hexagonal plate with its plane perpendicular to the trigonal z axis (all notation agrees with reference 4). It was therefore not difficult to orient the crystal with respect to its axis of suspension.

## 3. RESULTS

The principal measurements were performed on a 0.47-mg crystal distinguished by good uni-

\*The final form of the magnetic balance is described in detail in reference 6.

FIG. 1. The molar magnetic moment  $m$  as a function of magnetic field strength  $H$  for several temperatures: the five upper curves for  $H \perp z$ , the lowest curve for  $H \parallel z$ .



formity, while another crystal weighing 0.61 mg was used for a few control measurements. The absolute molar magnetic properties of the two crystals differed by 9%, which is included in the estimate of absolute experimental accuracy. All graphs shown below pertain to the 0.47-mg crystal, while the absolute values of constants in the text are averages for the two crystals.

As in the case of  $\text{MnCO}_3$ , measurements performed with the  $z$  axis of the samples parallel to the direction of suspension revealed no magnetic anisotropy in the basal plane. We therefore conclude, as in reference 4, that the anisotropy field for directions lying in the basal plane does not exceed 200 oe. Magnetic properties in a plane passing through the trigonal axis are shown in Figs. 1–4.

Figure 1 shows the measurements of the magnetic moment  $m$  as a function of the applied field  $H$  at several temperatures. It should be noted that when  $m_{\perp}$  was measured (with the field in the basal plane) the demagnetizing factor was zero, since the crystal plate was quite thin. The correction resulting from the demagnetizing factor ( $\sim 4\pi$ ) in measurements of  $m_{\parallel}$  (with the field perpendicular to the plate) amounts to  $\sim 1\%$  of the measured moment at  $T = 1.3^\circ\text{K}$  and decreases with decreasing  $\chi_{\parallel}$ . The torsion correction of  $m_{\parallel}(H)$  was obtained from measurements of  $\sigma_{\perp}$ ,  $\chi_{\perp}$ ,  $H$  and the torsion angle. Figure 1 shows that for  $H > 2$  koe the field dependence of the magnetic moments when  $T < T_N = 18.1^\circ\text{K}$  may be represented by

$$m_{\perp}(H, T) = \sigma(T) + \chi_{\perp}(T) H_{\perp}; \quad (1)$$

$$m_{\parallel}(H, T) = \chi_{\parallel}(T) H_{\parallel}. \quad (2)$$

Figure 2 shows how the projection  $m_H$  of the moment on the magnetic field direction depends on the angle between the field and the  $z$  axis. The solid curve, which was plotted assuming (1) and (2) to be valid for all field directions, is in good agreement with experiment; this indicates that the spontaneous moment  $\sigma$  always remains in the basal plane.

It must be mentioned that balance readings along the  $z$  axis in weak and moderate fields at  $T \leq 16^\circ\text{K}$  were very unsteady and that reproducibility was much less satisfactory than for measurements in the basal plane. We can therefore not arrive at a decision regarding the existence of

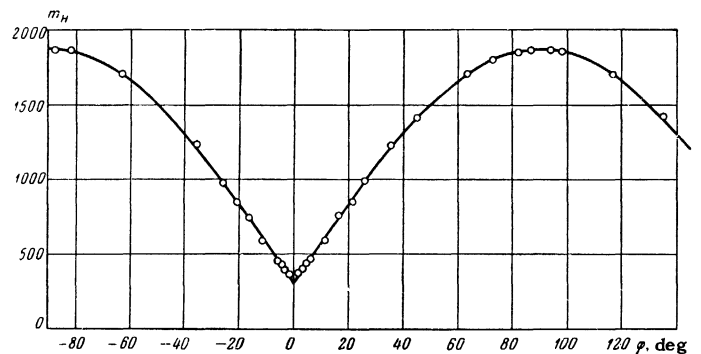


FIG. 2. Angular dependence of the projection of the moment on the magnetic field direction in the  $yz$  plane for  $H = 9480$  oe and  $T = 4.2^\circ\text{K}$ .  $\varphi$  is the angle between the field and the  $z$  axis. The solid curve is a plot of  $m(\varphi) = \chi_{\parallel} H + \sigma |\sin \varphi| + (\chi_{\perp} \chi_{\parallel}) H \sin^2 \varphi$ .

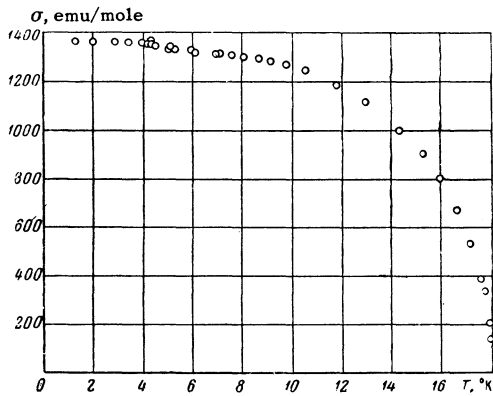


FIG. 3. Temperature dependence of the spontaneous ferromagnetic moment  $\sigma$ .  $T_N = (18.1 \pm 0.1)^\circ\text{K}$ ;  $\sigma_0 = (1440 \pm 75)$  cgs electromagnetic units per mole (average for the two crystals).

any anomaly of  $m_{||}$  (H) such as was detected for  $\text{MnCO}_3$ .<sup>4</sup>

Our experimental accuracy permits the statement that the spontaneous moment in the  $z$  direction does not exceed 25 cgs electromagnetic units per mole.

Curves similar to those in Fig. 1 were obtained for a considerable number of temperatures between 1.3 and  $19^\circ\text{K}$  and were treated graphically in order to yield values of  $\sigma(T)$ ,  $\chi_{\perp}(T)$  and  $\chi_{||}(T)$ . In the  $1.3$ – $8^\circ\text{K}$  region,  $\sigma(T)$  and  $\chi_{\perp}(T)$  were calculated from experimental data by least squares. The accuracy of  $\sigma(T)$  values was  $\pm 0.6\%$ . Anomalous behavior of  $\sigma(T)$  was observed below  $6^\circ\text{K}$  (Fig. 3). In order to verify whether the relatively sharp change of  $\sigma(T)$  near  $4.2^\circ\text{K}$  is associated with the change in the methods of maintaining temperatures above and below the helium boiling point, we performed a control experiment in which heating began in a bath at  $2.8^\circ\text{K}$ . The anomalous region of  $\sigma(T)$  was not affected.

Figure 4 shows values of  $\chi_{\perp}(T)$  and  $\chi_{||}(T)$ , relative measurements of which below  $100^\circ\text{K}$  were obtained with about  $0.4\%$  accuracy. At room temperature this was reduced to 1 and  $1.5\%$ , respectively, because of lower susceptibility. Fig. 4b shows that in the  $50$ – $300^\circ\text{K}$  region  $\chi_{\perp}$  obeys the Curie-Weiss law

$$\chi_{\perp} = C_{\perp}/(T - \Theta_{\perp}), \quad (3)$$

where  $C_{\perp} = 3.80 \pm 0.18^*$  and  $\Theta_{\perp} = -48 \pm 1^\circ$ . The behavior of  $\chi_{||}(T)$  above  $100^\circ\text{K}$  can be described by the same law with  $C_{||} = 4.00 \pm 0.25$  and  $\Theta_{||} = -215 \pm 5^\circ$ . The behavior of the principal susceptibilities at the transition point (Fig. 4a) exhibits a pronounced peak of  $\chi_{\perp}(T)$  and relatively little change of  $\chi_{||}(T)$ .

\*Values are given here and hereafter in cgs electromagnetic units per mole.

We are aware of two previous studies of the magnetic properties of  $\text{CoCO}_3$  at low temperatures,<sup>1,8</sup> in which polycrystalline samples were used. For a comparison with their results, above  $T_N$  we calculated  $\chi_p = \frac{2}{3}\chi_{\perp} + \frac{1}{3}\chi_{||}$  from our data. Because of small  $\chi_{||}$  it appears that  $\chi_p$  is also satisfactorily described by the Curie-Weiss law (3) with  $C_p = 3.6$  and  $\Theta_p = -63^\circ\text{K}$ .  $C_p$  is  $\sim 10\%$  greater in reference 1 and  $\sim 15\%$  smaller in reference 8 than in the present work. The agreement with reference 1 may be considered satisfactory if we take into account the authors' statement that their absolute values for  $\chi$  may have been reduced by  $\sim 10\%$  because of nonmagnetic impurities. It is difficult to make a quantitative comparison with the results obtained by Bizette,<sup>8</sup> who does not state the experimental values nor estimate the experimental error and sample purity. However, there is clear qualitative agreement.

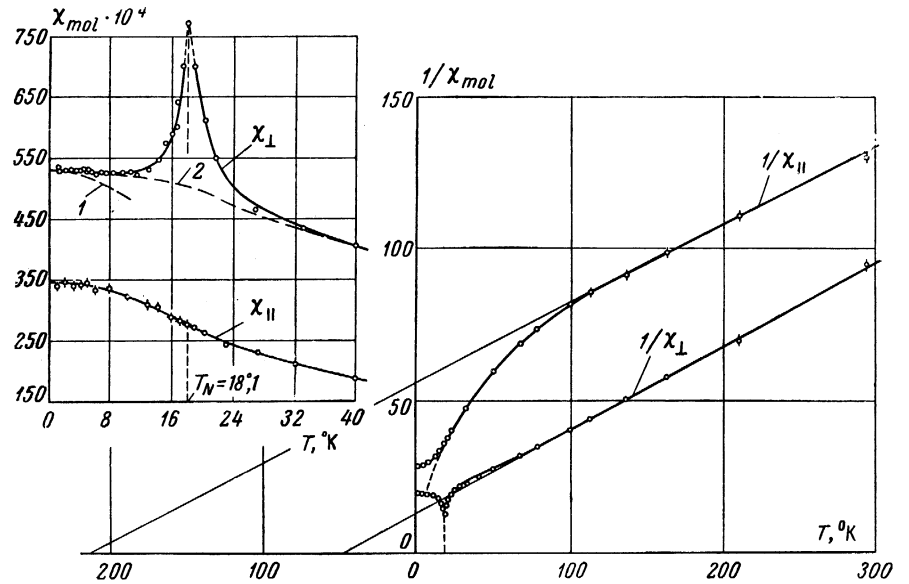
Bizette gives data only for temperatures above  $T_N$ . As already mentioned, the transition of  $\text{CoCO}_3$  to an antiferromagnetic state with weak ferromagnetism was first observed by one of the present authors and Orlova.<sup>1</sup> A small discrepancy in determining  $T_N$  ( $\sim 0.5^\circ$ ) may be associated with insufficient accuracy of thermocouple temperatures in reference 1, where measurements were confined to a very small temperature interval below  $T_N$ , so that values of  $\sigma$  cannot be compared.

#### 4. DISCUSSION OF RESULTS. DEVELOPMENT OF THE THERMODYNAMIC THEORY OF WEAK FERROMAGNETISM

1. In agreement with preliminary results obtained using polycrystalline samples<sup>1</sup> and with thermodynamic theory,<sup>3</sup> our results have established that a  $\text{CoCO}_3$  single crystal becomes antiferromagnetic with weak ferromagnetism below  $T_N = 18.1^\circ\text{K}$ . As in the case of  $\text{MnCO}_3$ ,<sup>4</sup> the ferromagnetic moment  $\sigma$  always remains in the basal plane but is almost 10 times larger than in  $\text{MnCO}_3$ . For  $T \rightarrow 0$  we have  $\sigma \rightarrow 1440$  cgs emu/mole. Differences in the behavior of the two crystals will be discussed in detail below.

2. In the paramagnetic region ( $T \gg T_0$ ) the susceptibility of  $\text{CoCO}_3$  exhibits very large anisotropy ( $\sim 30\%$  at  $T = 300^\circ\text{K}$ ). Anomalously large anisotropy has also been observed in other cobalt compounds, both in the case of a strong exchange interaction ( $\text{CoF}_2$ ,  $\text{CoSO}_4$ ) and in the case of dilute salts with weak interaction. In a number of theoretical papers (such as reference 9) this anisotropy has been attributed to the anomalous splitting of the orbital septet in the ground state

FIG. 4. Temperature dependence of the magnetic susceptibility of  $\text{CoCO}_3$  in the paramagnetic and antiferromagnetic states. Curve 1 – from spin-wave theory; curve 2 – smooth interpolation through the transition region.



( $^4F_{9/2}$ ) of a free cobalt ion in the crystalline field. It was assumed that, in contrast with other ions of the iron group, in first approximation (a cubic field) when splitting into a singlet and two triplets occurs, a triplet level is split by the axially approximation this level is split by the axially symmetric crystalline field and spin-orbit interaction into six Kramers doublets. The specific scheme of these doublets should account for the following experimental features which we observed in the behavior of  $\chi_{\perp}$  and  $\chi_{\parallel}$ : the large difference between  $\chi_{\parallel}$  and  $\chi_{\perp}$ , the approximate equality of  $C_{\parallel}$  and  $C_{\perp}$  above  $100^{\circ}\text{K}$  and the sharp departure of  $\chi_{\parallel}$  from the Curie-Weiss law below  $100^{\circ}\text{K}$ . However, these experimental facts are insufficient for determining the level scheme uniquely. In any event it is evident that the orbital moment makes a large anisotropic contribution to the magnetic properties of  $\text{CoCO}_3$ .

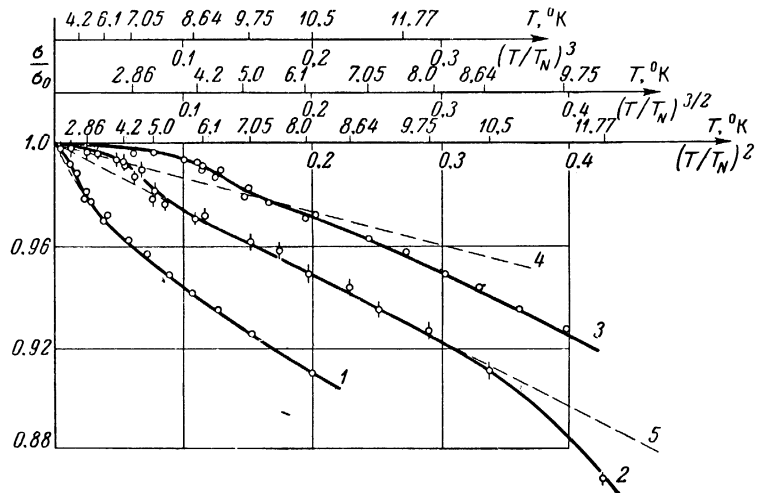
3. At very low temperatures ( $T \ll T_N$ ) it is

interesting to compare our results with spin-wave theory. The phenomenological theory of spin waves as applied to rhombohedral antiferromagnetics with weak ferromagnetism<sup>4,10</sup> yields the following conclusions. In this case the spin-wave spectrum consists of two branches, one of which exhibits the energy gap  $kT_{AE} = \mu\sqrt{2H_A H_E}$  ( $H_A$  and  $H_E$  are the effective fields of anisotropy and spatial interaction, respectively). The other branch contains no gap and in the absence of an external field is of the phonon type. When  $T \ll T_{AE}$  only the latter branch is excited. For the temperature dependence of  $\sigma$  and  $\chi_{\perp}$  we then obtain

$$\sigma = \sigma_0 \{1 - \eta(T/T_N)^2\}, \quad \chi_{\perp} = \chi_{\perp}^0 \{1 - 2\eta(T/T_N)^2\}. \quad (4)$$

When  $T \gg T_{AE}$  both branches are excited. The law for the variation of  $\chi_{\perp}$  then remains unchanged, but  $\sigma$  begins to decrease twice as rapidly:

FIG. 5. Dependence of the relative ferromagnetic moment  $\sigma/\sigma_0$  on the reduced temperature  $T/T_N$ . Curve 1 – for the cubic scale; curves 2, 4, 5 – for the quadratic scale; curve 3 – for the 3/2 scale. Curves 4 and 5 are theoretical spin-wave plots [see (4) and (5)].



$$\sigma = \sigma_0 \{1 - 2\eta(T/T_N)^2\} \text{ for } T_{AE} \ll T \ll T_N. \quad (5)$$

In the region of  $T \sim T_{AE}$  an anomaly associated with the transition from (4) to (5) should appear in the behavior of  $\sigma(T)$ . In the case of  $\text{MnCO}_3$  this region was below the investigated temperatures ( $T_{AE} < 1.5^\circ\text{K}$ ).<sup>4</sup> In the case of  $\text{CoCO}_3$  the transition region was in the accessible temperature range, as is shown in Fig. 5, where the experimental behavior of  $\sigma/\sigma_0$  is compared with (4) and (5). The values of  $\sigma/\sigma_0$  are plotted for three temperature scales — cubic, quadratic and semicubic. For 5–10°K, in agreement with (5), the experimental points fit well on a straight line passing through the point (0;1) only for the quadratic scale. This was used to determine  $2\eta = 0.26 \pm 0.2$  in (5). In the vicinity of 4.5°K the temperature dependence of  $\sigma/\sigma_0$  exhibits the changed behavior that is predicted by theory for the  $T_{AE}$  region. Thus  $T_{AE} \sim 4^\circ\text{K}$  for  $\text{CoCO}_3$ . Our experiments were insufficiently accurate to confirm that at lower temperatures  $\sigma/\sigma_0$  approaches unity in accordance with the first equation in (4) (curve 4 in Fig. 6). However, there is no experimental disagreement with this equation.

Figure 4a compares the experimental behavior of  $\chi_\perp(T)$  with the second equation in (4) (curve 1). As in the case of  $\text{MnCO}_3$ , experimental values of  $\chi_\perp$  do not fall off as rapidly as is required by the spin-wave theory. The results obtained for  $\text{CoCO}_3$  confirm our earlier conclusion that the existing theory of spin waves is incomplete.<sup>4</sup>

4. Our most interesting result is the broad high peak of  $\chi_\perp(T)$  in the vicinity of  $T_N$ , similar to that observed for  $\text{MnCO}_3$ ,<sup>4</sup> although the latter peak was very small. As already stated,  $\text{CoCO}_3$  is distinguished by an unusually large contribution of the spin-orbit interaction to the anisotropy energy. This is confirmed by the large ferromagnetic moment  $\sigma$ ; it was shown in references 5 and 6 that the dipole interaction does not produce weak ferromagnetism in rhombohedral structures. The thermodynamic theory will be used below to show that the broad peak of the perpendicular susceptibility is also associated with large anisotropy energy.

5. According to the thermodynamic theory of antiferromagnetism,<sup>3</sup> the thermodynamic potential for rhombohedral crystals such as  $\text{MnCO}_3$  and  $\text{CoCO}_3$  (symmetry group  $D_{3d}^6$ ) near the transition point is

$$\begin{aligned} \tilde{\Phi} = & \frac{1}{2}(Al^2 + Bm^2 + al_z^2 + bm_z) \\ & + \beta(l_x m_y - l_y m_x) + \frac{1}{4}Cl^4 + \frac{1}{2}Dl^2 m^2 - mH. \end{aligned} \quad (6)$$

Here  $\mathbf{l} = \mathbf{M}_1 - \mathbf{M}_2$  is the antiferromagnetic vector,

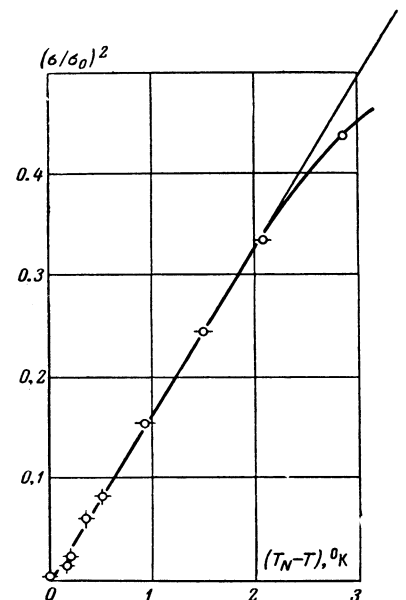


FIG. 6. Temperature dependence of the square of relative spontaneous magnetization near the transition point.

$\mathbf{m} = \mathbf{M}_1 + \mathbf{M}_2$  is the magnetic moment of the crystal, and  $\mathbf{M}_1$  and  $\mathbf{M}_2$  are the magnetizations of the sublattices.

We shall hereinafter be interested only in the state with weak ferromagnetism where  $\mathbf{l}$  lies in the basal plane ( $a > 0$ ). Dzyaloshinskiĭ has shown<sup>3</sup> that when not too small magnetic fields  $\mathbf{H}$  are applied to the basal plane\* we always have  $\mathbf{l} \perp \mathbf{m}$  and  $\mathbf{m} \parallel \mathbf{H}$ , so that the thermodynamic potential can be expressed, without affecting its generality, as

$$\tilde{\Phi} = \frac{1}{2}Al^2 + \frac{1}{4}Cl^4 + \frac{1}{2}Bm^2 - \beta m l - mH^\dagger. \quad (7)$$

We have here omitted the term  $\frac{1}{2}Dl^2 m^2$  which would change  $\chi_\perp$  by only a few percent,<sup>4</sup> whereas the anomaly of interest amounts to some tens percent.

In the absence of a magnetic field ( $H = 0$ ) the conditions for minimizing  $\tilde{\Phi}$  are

$$\begin{aligned} \partial\tilde{\Phi}/\partial l &= Al - \beta m + Cl^3 = 0, \\ \partial\tilde{\Phi}/\partial m &= -\beta l + Bm = 0, \end{aligned} \quad (8)$$

which show that the temperature for a transition to an ordered state ( $l \neq 0$ ;  $m \neq 0$ ) is determined by the condition that the determinant of equations which are homogeneous in  $l$  and  $m$  shall equal zero:  $AB - \beta^2 = 0$ . Near  $T_N$  we therefore have,

\*For  $\chi_{\parallel}$  our subsequent consideration of the anisotropy energy ( $\beta$ ) leads to no new result; therefore the equations in references 3 and 4 for the temperature dependence of  $\chi_{\parallel}$  remain valid.

†In a state of equilibrium the relative orientation of the vectors  $\mathbf{l}$  and  $\mathbf{m}$  is such that the term  $-\beta m l$  is always less than zero.

as usual,

$$A - \beta^2/B = \nu(T - T_N). \quad (9)$$

In Dzyaloshinskiĭ's calculations<sup>3</sup> the term  $\beta m$  in (8) was omitted and the condition for the transition to the antiferromagnetic state was  $A = 0$ . Inclusion of this term is seen to shift the transition point by the amount  $\beta^2/\nu B$ . In the case of  $\text{CoCO}_3$  estimates of the coefficients (see below) show that this shift amounts to  $\sim 0.5^\circ$ .

6. It is more important to include the same term in the presence of a magnetic field ( $H \neq 0$ ), in which case the minimization of  $\tilde{\Phi}$  is represented by

$$Al - \beta m + Cl^3 = 0, \quad -\beta l + Bm = H. \quad (10)$$

When  $T > T_N$  we have small  $l$  and the term  $Cl^3$  may be neglected if  $T$  is not too close to  $T_N$  (the range of applicability of this approximation is given below). In view of (9) solutions of (10) then provide formulas for the temperature and field dependencies of  $l$  and  $m$ :

$$l = \beta H / B\nu(T - T_N), \quad (11)$$

$$m = [1/B + \beta^2/B^2\nu(T - T_N)] H. \quad (12)$$

(11) shows that in the given case antiferromagnetic ordering is induced by a magnetic field even above  $T_N$ . For antiferromagnets with weak ferromagnetism, as for exchange ferromagnets,  $T_N$  is therefore an isolated second-order transition point in the  $H$ - $T$  plane.

(12) shows that the magnetic moment  $m$  varies linearly with the field, but  $\chi_\perp$  must increase steeply as  $T_N$  is approached.

7. For  $T < T_N$  antiferromagnetic ordering exists in the absence of a field, so that the term  $Cl^3$  cannot be neglected. The second equation in (10) gives

$$m = (\beta l + H)/B, \quad (13)$$

and after substitution for  $m$  in the first equation we obtain the following cubic equation in  $l$ :

$$BCl^3 + B\nu(T - T_N)l - \beta H = 0. \quad (14)$$

The zeroth approximation in  $\beta$ , as in the absence of a field, gives

$$l_0^2 = (\nu/C)(T_N - T). \quad (15)$$

The first approximation for  $l$  will be sought in the form  $l = l_0 + X\beta$ . Assuming a weak field (see below) and dropping terms containing  $\beta^2$  and  $\beta^3$ , after substitution in (14) we obtain

$$l = [(\nu/C)(T_N - T)]^{1/2} + \beta H/2B\nu(T_N - T). \quad (16)$$

Thus a field here also increases antiferromagnetic ordering.

With the dependence of  $l$  on  $H$  and  $T$  known, (13) gives for  $m$  the same formula containing the spontaneous moment as in reference 3:

$$m = \sigma + \chi_\perp H, \quad (17)$$

where

$$\sigma = \beta l_0/B = [\beta^2\nu(T_N - T)/B^2C]^{1/2}, \quad (18)$$

$$\chi_\perp = 1/B + \beta^2/2B^2\nu(T_N - T). \quad (19)$$

The temperature dependence of  $\sigma$  is the same as in reference 3. However, (12) and (19) show that magnetically induced ordering results in equations that predict a sharp rise of  $\chi_\perp$  as  $T_N$  is approached from either direction.

8. As already indicated, the equations derived above are valid for not very strong fields and at temperatures that are close but not too close to the transition temperature [so that (8) and (9) will hold true]. The limitation on the closeness to  $T_N$  is associated with the necessity of observing the inequality  $Cl^3 \ll \beta H/B$  (for  $T > T_N$ ) and the possibility of dropping terms containing  $\beta^2$  and  $\beta^3$  in solving (14) (for  $T < T_N$ ). The estimates of the interval  $\Delta T$  near  $T_N$  where the derived equations cease to be satisfied almost coincide in both instances at the value

$$\Delta T \approx (\beta^2 CH^2/B^2\nu^3)^{1/2}.$$

Using the values of the expansion coefficients given below, we obtain  $\Delta T \approx 0.5^\circ$  for the maximum applied fields. For  $|T - T_N| \lesssim \Delta T$  the expression for  $l$  contains terms which leave the derivative  $\partial m/\partial H$  in  $T_N$  finite and lead to the field dependence of  $\chi_\perp$ .

9. Good qualitative agreement is found between the experimental temperature dependence of  $\chi_\perp$  (Fig. 4a) and (12) and (19). For the purpose of a rough quantitative comparison we interpolated a curve which smooths out the peak at  $T_N$  (curve 2 in Fig. 4a), and plotted the temperature dependence of the reciprocal of  $\Delta\chi = \chi_\perp - (\chi_\perp)_{\text{interp}}$ . The resulting points could be satisfied by two straight lines intersecting at  $T_N$ , with slopes differing by a factor of about 2 in accordance with theory. This led to the estimate  $(B^2/\beta^2)\nu = 40$ .

The experimental temperature dependence of  $\sigma$  near  $T_N$  and a plot of (18) are shown in Fig. 6.  $(\sigma/\sigma_0)^2$  is seen to depend linearly on  $T_N - T$  up to  $\sim 2.5^\circ$  from  $T_N$  and down to  $\sigma/\sigma_0 \sim 0.6$ . We thus determine  $\xi = \beta^2\nu T_N/B^2\nu\sigma_0^2 = 3.0$ .

The foregoing experimental results enabled us

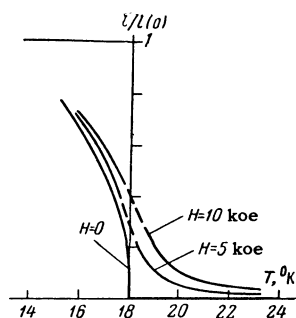


FIG. 7. Theoretical dependence of the antiferromagnetic vector  $l$  on  $T$  and  $H$  near  $T_N$  (the transition point in zero field).

to estimate the expansion coefficients of the thermodynamic potential (7):  $B = 18$ ;  $\beta = 1.5$ ;  $\nu = 0.25$ ;  $C = 4.5 \times 10^{-9}$ . In calculating  $\beta$  we assumed that at  $T = 0^\circ\text{K}$  we have  $l_0 = 16.75 \times 10^3$  (only the spin moment).

10. The values obtained for the coefficients permit a quantitative estimate of the antiferromagnetic ordering induced in  $\text{CoCO}_3$  by an applied magnetic field. Figure 7 shows the temperature dependence of relative magnetization in antiferromagnetic sublattices for different fields as calculated according to (11) and (16). An effect of considerable magnitude should be exhibited by  $\text{CoCO}_3$  in relatively weak fields and could presumably be detected directly by either the neutron diffraction or nuclear resonance technique for measuring antiferromagnetic ordering.

The authors are very grateful to Academician P. L. Kapitza for his continued interest, and also wish to thank I. E. Dzyaloshinskiĭ for valuable

discussions, N. M. Kreĭnes for methodological discussions and N. Yu. Ikornikova for preparation of the single crystals. The experimental assistance of V. I. Kolokol'nikov is also gratefully acknowledged.

<sup>1</sup>A. S. Borovik-Romanov and M. P. Orlova, JETP 31, 579 (1956), Soviet Phys. JETP 4, 531 (1957).

<sup>2</sup>P. A. Alikhanov, JETP 36, 1690 (1959), Soviet Phys. JETP 9, 1204 (1959).

<sup>3</sup>I. E. Dzyaloshinskiĭ, JETP 32, 1547 (1957), Soviet Phys. JETP 5, 1259 (1957).

<sup>4</sup>A. S. Borovik-Romanov, JETP 36, 766 (1959), Soviet Phys. JETP 9, 539 (1959).

<sup>5</sup>F. Bertaut, Compt. rend. 246, 335 (1958).

<sup>6</sup>A. S. Borovik-Romanov, Dissertation, Institute for Physical Problems, Acad. Sci. U.S.S.R., 1959.

<sup>7</sup>A. S. Borovik-Romanov and N. M. Kreĭnes, JETP 29, 790 (1955), Soviet Phys. JETP 2, 657 (1956).

<sup>8</sup>H. Bizette, Ann. phys. 1, 233 (1946).

<sup>9</sup>A. Abragam and M. H. L. Pryce, Proc. Roy. Soc. (London) A206, 173 (1951).

<sup>10</sup>E. A. Turov, JETP 36, 1254 (1959), Soviet Phys. JETP 9, 890 (1959).

Translated by I. Emin